

NEW DIAGNOSTICS AND CURES FOR COUPLED-BUNCH INSTABILITIES

S. Prabhakar*, Dept. of Mathematics, Stanford, CA 94305

J.D. Fox and D. Teytelman, Stanford Linear Accelerator Center, Stanford, CA 94309

Abstract

As circular accelerators move towards larger numbers of bunches and higher beam currents, the task of diagnosing and curing coupled-bunch instabilities becomes ever harder. This paper describes the use of phase space tracking, *i.e.* reconstruction of bunch phase space trajectories, as a comprehensive instability diagnostic. A new instability cure is also presented, based on recent insights into the dynamics of unevenly-filled rings. Data is shown from PEP-II and the ALS, where “optimally shaped” uneven fills have yielded significant increases in instability thresholds.

1 INTRODUCTION

Modern synchrotron light sources and circular colliders must store high-current charged-particle beams to meet their design goals. The most serious consequence of high currents is the possibility of collective instabilities, which result from self-amplifying electromagnetic interactions between the beam and its surroundings [1]. In the new machines, beam current is typically distributed among large numbers of circulating bunches, so as to avoid single-bunch instabilities, improve the beam lifetime, and reduce two-beam effects (in the case of colliders). Consequently, unstable coupling between bunches through long-range wake fields is often the main current-limiting factor.

An N -bunch beam has N modes of coupled-bunch oscillation. Thus, modern accelerators have hundreds or thousands of potentially unstable modes. This makes instability diagnosis by conventional techniques quite difficult. During commissioning, beam conditions are often rapidly varying and poorly characterised, and during regular operation, not much time is available for diagnostic experiments. There is a real need for quicker and more informative measurement and analysis techniques, which must be complemented by imaginative ways of damping coherent motion.

Section 2 describes an instability diagnostic that utilises phase space trajectories reconstructed from measured beam-position signals. In addition to enabling estimation of coherent tunes and bunch tunes with accuracy of a few Hz, phase space tracking allows new kinds of comparisons between instability theory and experiment. Such comparisons are shown to be useful in distinguishing between the fast beam-ion instability (FBII) [2, 3] and conventional instabilities in the PEP-II High Energy Ring (HER).

The theory of coupled-bunch instabilities in even fills (constant bunch spacing, bunch currents) is well under-

stood [4, 5]. Unfortunately, there is no general analytic solution for the eigenvalues (growth rates and coherent tune shifts) of an uneven fill, though there have been useful insights into some special cases [6, 7, 8, 9].

In practice, empirically selected uneven fills have successfully raised instability thresholds at the Cornell Electron Storage Ring [10], the SPEAR storage ring [11], the Advanced Photon Source [12], and a few other machines. Recently, the longitudinally stabilising effect of interbunch tune spreads, arising from RF cavity transients induced by gaps in the fill, has been noted [8, 13].

The following problem is addressed in Section 3: given an effective beam impedance $Z^{eff}(\omega)$ and a maximum allowable bunch current i_{max} , how does one distribute the desired beam current I_o among the h RF buckets to minimise the largest instability growth rate $\max_l [Re(\lambda_l)]$? Solutions to this problem are presented in terms of two physical phenomena that underlie uneven-fill dynamics: modulation coupling of even-fill eigenmodes (EFEMs) and fill-induced Landau damping. The term Landau damping refers to damping of coherent oscillations via a spread in the resonant frequencies of individual oscillators [14].

All of the experiments shown in this paper were performed with the help of a programmable longitudinal feedback (LFB) system, which can digitise and store the oscillation coordinate of each bunch while simultaneously manipulating feedback parameters [15, 16].

This paper condenses Chapters 5 and 7 of [17].

2 PHASE SPACE TRACKING

The LFB system has been used to record data on longitudinal and transverse instabilities at various accelerators. A typical piece of data consists of the downsampled oscillation signals of all the bunches over a few tens of ms.

The measured position signal s_n^k of bunch k (n is the sample number) is taken to be the x-coordinate in phase space. The y-coordinate is usually a scaled version of the time-derivative $\dot{s}^k(t)$, sampled at the same instants. However, for the purpose of estimating tunes and growth rates, it is more convenient to calculate the y-coordinate by phase-shifting the signals s_n^k by 90° [18]. Thus, what is referred to in this paper as the “phase space trajectory” is more accurately termed the *analytic signal trajectory* in the complex plane. In practice, the difference is very small because bunch oscillations are usually narrowband.

The Cartesian phase space coordinates can be converted to magnitude-and-phase coordinates a_n^k and ϕ_n^k . The instantaneous growth rate is $\frac{1}{a} \frac{da}{dt}$, and the instantaneous os-

* shyam@stanford.edu

cillation frequency is $\frac{d\phi}{dt}$.

A low-threshold vertical instability that showed up in the PEP-II HER during commissioning was initially suspected to be an FBII. Numerous experiments were performed to confirm this hypothesis, or alternatively, to confirm the competing hypothesis of an unexpectedly large impedance resonance somewhere in the ring. These included studies of the effects of variations in gas pressure, bunch spacing, train length, and bunch currents on the spectrum of betatron sidebands. These studies did not always give consistent results, because conditions such as beam orbit, vacuum pressure, coupling, beam size, feedback state, etc. were sometimes not well controlled during commissioning.

In such cases, we require a diagnostic that is based on a single measurement (insensitive to parameter drift), and can be interpreted without knowledge of factors such as beam size, vacuum pressure, etc. Phase space tracking fills this need by enabling measurement of tune and growth-rate variation along a bunch train. The FBII is expected to produce exponential growth and linear variation of growth rates and tune shifts along a short bunch train [19].

The vertical instability was investigated using a digitised record of the exponentially growing oscillations of each bunch, immediately after switching off feedback. The 150-bunch train had a 4.2 ns spacing and $I_o = 52$ mA. Phase space trajectories were constructed from the data, and growth rates and tune shifts were calculated using curve fitting.

Figure 1(a) shows the fitted tunes of bunches 46 to 150, relative to the tune of bunch 150. The peak-to-peak variation is less than 50 rad/s. The first 45 bunches were excluded because they grew to smaller amplitudes and had smaller signal-to-noise ratios. The growth rates are shown in Fig. 1(b). As can be expected of conventional instabilities, the growth rate variation across the train is small enough to be accounted for by the presence of secondary eigenmodes at small amplitudes. Clearly, growth rates and tunes do not vary linearly with bunch number. As a result, the FBII hypothesis was deemed improbable. It is of course possible that some of the approximations made in [19] do not apply to the relative time scales of this experiment.

The hypothesis that best fits the results of various experiments performed to find the source of this instability is that the beam was driven by a large impedance in the interaction region (IR), which disappeared after subsequent changes to the shape of the IR [20].

3 CURING INSTABILITIES WITH UNEVEN FILLS

The most direct approach to solving the uneven-fill eigenvalue problem is numerical computation of the eigenvalues of the $N \times N$ bunch coupling matrix [21]. Alternatively, one could project the coupled-bunch motion onto the N EFEMs, and calculate the “modal” coupling matrix [22].

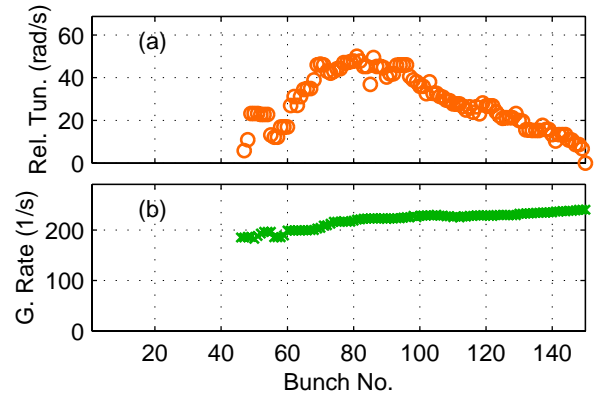


Figure 1: (a) Relative tunes of bunches 46 to 150, calculated using linear fits to the phase space angle signals of the bunches. (b) Growth rates of the same bunches, from exponential fits to the magnitude transients a^k .

3.1 Derivation of Modal Coupling Matrix

Due to azimuthal symmetry, the N Fourier vectors $v_l = [1 e^{jl\theta} e^{2jl\theta} \dots e^{(N-1)jl\theta}]^T$; $\theta = 2\pi/N$; $l = 0, \dots, N-1$, make up the eigenmodes of an N -bunch even fill. In the absence of wake fields, all modes have the same eigenvalue $-d_r + j\omega_s$, where d_r is the radiation damping rate and ω_s is the longitudinal oscillation frequency. From here on, we shall use the word “eigenvalue” only for the coherent eigenvalue shift produced by wake fields.

In the general case, the longitudinal arrival-time error τ_n of the n^{th} bunch centroid is given by

$$\ddot{\tau}_n + 2d_r \dot{\tau}_n + \omega_s^2 \tau_n = -\frac{\alpha e}{ET_o} V_n, \quad (1)$$

where α is the momentum compaction factor, E/e is the nominal beam energy in Volts, $T_o = 2\pi/\omega_o$ is the revolution period, and $V_n(t)$ is the total wake voltage seen by bunch n . If the bunches are much shorter than relevant impedance wavelengths,

$$V_n(t) = \sum_{p=-\infty}^{\infty} \sum_{k=0}^{N-1} q_k W[t_{n,k}^p + \tau_n(t) - \tau_k(t - t_{n,k}^p)],$$

where q_k is the charge of bunch k , $t_{n,k}^p = (n - k - pN)T_b$, T_b is the bunch spacing (T_o/N), and the longitudinal wake function $W(t)$ equals zero when $t < 0$. The total ring impedance is $Z(\omega) = \int_{-\infty}^{\infty} W(t)e^{-j\omega t} dt$.

We shall now switch to the following modal (EFEM) basis: $\nu_m = \sum_{n=0}^{N-1} \tau_n e^{-j2\pi \frac{mn}{N}}$, $\tau_n = \frac{1}{N} \sum_{m=0}^{N-1} \nu_m e^{j2\pi \frac{mn}{N}}$. This is a natural basis for studying fill shape effects. We assume eigenmodes of the form $\tau_k = B_k e^{j\Omega t}$; $k = 0, \dots, N-1$. Similarly, $\nu_m = D_m e^{j\Omega t}$; $m = 0, \dots, N-1$. If $d_r \ll \omega_s$ and $|\Omega - \omega_s| \ll \omega_s$, the projection of τ and V onto the l^{th} EFEM gives:

$$\dot{\nu}_l + (d_r - j\omega_s)\nu_l = \frac{\alpha e f_{rf}}{2EQ_s} \sum_{m=0}^{N-1} I_{l-m} Z_{lm}(\omega_s) \nu_m$$

$$= \sum_{m=0}^{N-1} A_{lm} \nu_m, \quad (2)$$

where f_{rf} is the RF frequency, $Q_s = \omega_s/\omega_o$ is the tune, and the amplitude of the p^{th} revolution harmonic in the beam spectrum is $I_p = \sum_{k=0}^{N-1} i_k e^{-j2\pi \frac{pk}{N}}$; $i_k = q_k/T_o$.

$$\begin{aligned} Z_{lm}(\omega) &= Z^{eff}(l\omega_o + \omega) - Z^{eff}[(l-m)\omega_o]; \\ Z^{eff}(\omega) &= \frac{1}{\omega_{rf}} \sum_{p=-\infty}^{\infty} (pN\omega_o + \omega) Z(pN\omega_o + \omega) \end{aligned} \quad (3)$$

If the fill is even, $I_k = 0$ for $k \neq 0$, and the off-diagonal elements of the coupling matrix A disappear. The diagonal terms yield the well-known equations [5] for even-fill eigenvalues: $\lambda_l = \frac{\alpha e f_{rf}}{2EQ_s} I_o Z^{eff}(l\omega_o + \omega_s)$; $l = 0, \dots, N-1$. Most commonly-used fill shapes are close to even ($I_k/I_o \approx 0$ for most k). Also, Z_{lm} has the same order of sparseness as Z^{eff} . Since the off-diagonal terms are proportional to $I_{l-m} Z_{lm}$, it is apparent from Eq. (2) that the EFEM basis makes A sparse. In other words, the A -matrix is sparse unless both I_k and Z^{eff} are dense, which is not a very common situation.

3.2 Modulation Coupling

Modulation coupling arises from terms of the form $I_{l-m} Z^{eff}(l\omega_o + \omega_s)$, which reflect the fact that the longitudinal beam signal is proportional to $i_k \tau_k$, the modulation product of the fill shape and bunch position signals. For example, assume that the bunches oscillate in EFEM p , and consequently, the bunch position signal has a frequency component $p\omega_o + \omega_s$. If the fill shape has a sinusoidal component at $q\omega_o$ (I_q is nonzero), then the beam signal has spectral lines at $(p \pm q)\omega_o + \omega_s$. Thus, modulation by the fill shape causes coupling between EFEMs p and $(p \pm q)$.

If $I_k Z^{eff}(k\omega_o)$ is negligible for all $k \neq 0$, the modulation coupling terms are the only manifestation of fill unevenness. In addition, if $Z(\omega)$ is non-negligible only at n revolution harmonics, where $n \ll N$, we can approximate the most unstable eigenvalues by those of an equivalent A -matrix consisting only of the n corresponding rows and columns. This is a great simplification in large rings with hundreds or thousands of bunches. If we now create a fill so that only I_{l-m} is large, where EFEM l is the most unstable mode and m is the most stable, we get an equivalent A -matrix that is diagonal except for the coupling between ν_m and ν_l . This reduces the eigenvalue problem to a quadratic equation with the solution:

$$\lambda = \frac{1}{2}(\lambda_l + \lambda_m) \pm \frac{1}{2} \sqrt{(\lambda_l - \lambda_m)^2 + 4C_{l-m}^2 \lambda_l \lambda_m}, \quad (4)$$

where C is a modulation parameter defined by $C_p = |I_p|/I_o$. If $C_{l-m} = 0$, the even-fill eigenvalues λ_l and λ_m are unperturbed. As C_{l-m} approaches unity (it can never exceed 1), one eigenvalue approaches zero and the other approaches $\lambda_l + \lambda_m$. This yields the maximum damping.

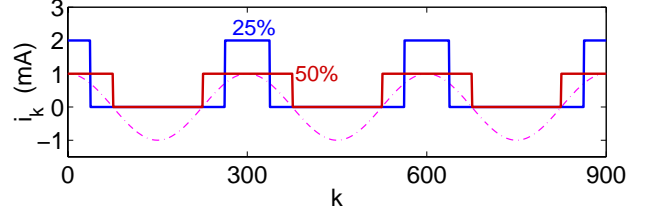


Figure 2: Example of fill optimisation. $h = 900$, $I_o = 450$ mA. Solid lines: 50% fill and 25% fill maximise C_3 for $i_{max} = 1$ mA, 2 mA. Dashdot: Reference sinusoid at $3\omega_o$.

Algorithm for Optimising Fill Shape It can be shown that the following algorithm maximises C_p , given the beam current I_o and the maximum allowable bunch current i_{max} : 1) For each bucket n in the N -bucket pattern, calculate a corresponding “weight” $\cos(2\pi \frac{pn}{N})$. 2) Pick the B buckets with the highest weight, and fill each of them to the same current i_{max} , where $B = I_o/i_{max}$. Leave the remaining buckets empty.

Figure 2 shows two example fills which maximise C_3 when $h = 900$, $I_o = 450$ mA, and $i_{max} = 1$ mA, 2 mA.

3.3 Fill-induced Landau Damping

The second important uneven-fill phenomenon is potential-well distortion that varies from bucket to bucket, causing bunch-to-bunch tune variation and Landau damping. Fill-induced Landau damping arises from terms of the form $I_{l-m} Z^{eff}[(l-m)\omega_o]$ in Eq. (2). The tune shift of bunch k relative to the mean tune is

$$\delta\omega_s^k = j \frac{\alpha e f_{rf}}{2EQ_s} \sum_{l=1}^{N-1} \left[I_l Z^{eff}(l\omega_o) e^{j2\pi kl/N} \right] \quad (5)$$

$\delta\omega_s$ is purely real, since the real part of the summand is an odd function of l , with period N . All unstable modes are damped by the interbunch tune spread.

If n is the most unstable EFEM, Eq. (5) indicates that a good strategy would be to design a fill that optimises $C_n = |I_n|/I_o$. The best value of C_n for damping EFEM n is different from the optimum for other EFEMs:

A) Landau damping of EFEMs other than n can be calculated in the usual way [14], if they are not coupled to other prominent EFEMs by modulation coupling or by tune-spread terms on the n^{th} diagonal of A .

B) Damping of EFEM n is larger than that of other modes, since the combination of tune spread and fill unevenness introduces coupling between ν_n and ν_{N-n} . If Landau damping and coupling to ν_{N-n} are the only significant effects and $\lambda_{-n} \approx -\lambda_n^*$ [23], then the variation of λ_n with fill fraction is shown in Fig. 3 (numerical computation, assuming use of the fill optimisation algorithm). This figure is symmetric about both axes. Dashed lines show the evolution of λ_n from a few even-fill starting points. Interestingly, in this special case, fill unevenness only seems to

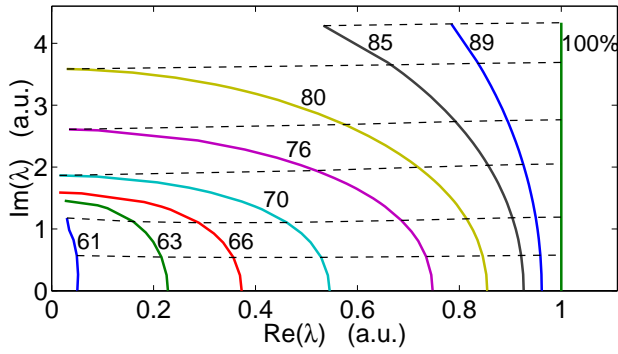


Figure 3: Graphical look-up table for fill-induced damping of unstable longitudinal eigenvalue λ_n as C_n is increased from 0 (100% of ring filled) to 0.5 (61% filled). Dashed lines: Evolution of λ_n from a few even-fill starting points.

reduce the growth rate $Re(\lambda)$, without changing the coherent tune $Im(\lambda)$ very much. EFEM n is best damped by maximising C_n , *i.e.*, by minimising the fill fraction.

3.4 Expt. Verification: Modulation Coupling

Figure 4(a) shows the estimated cavity-induced growth rates in the PEP-II Low Energy Ring (LER) at the nominal bunch spacing of 8.4 ns ($N = 873$), when $I_o = 1$ A. The estimate is based on offline cavity measurements [24]. The two largest cavity resonances are expected to drive bands of modes centered at 93.1 MHz (EFEM 683) and 105 MHz (EFEM 770) unstable. They also stabilise corresponding bands at 25.9 MHz (EFEM 190) and 14 MHz (EFEM 103). Here the best modulation-coupling cure would be to couple the modes around 105 MHz to those near 25.9 MHz by maximising C_{580} , *i.e.*, C_{293} ($C_p = C_{N-p}$). This automatically couples 93.1 MHz to 14 MHz. In general, if ν_a couples to ν_{N-b} , then ν_b couples to ν_{N-a} . Maximising C_{291} should work as well, since ω_o is small compared to the bandwidths of the resonances. This is easily achieved by filling every third nominally-spaced bucket, since $291 = 873/3$. The calculation illustrated in Fig. 4(b) shows that such a fill should be stable at 1 A.

Modulation coupling was expected to raise the instability threshold from 305 mA (nominal spacing) to 1.16 A ($3 \times$ nominal spacing). The measured thresholds are 350 mA and 660 mA respectively. The improvement is significant, though smaller than expected, probably because the impedance resonances are located 3-5 MHz away from their expected positions. Given our new knowledge of the higher order mode resonant frequencies, it seems likely that a bunch spacing of 11 RF buckets would have resulted in even better damping.

3.5 Expt. Verification: Landau Damping

Theoretical predictions of fill-induced Landau damping were first tested at the ALS, where the diagnostic capabilities of a digital longitudinal feedback system [15, 16] were

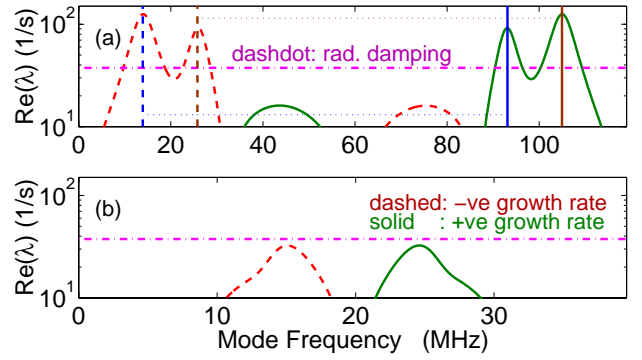


Figure 4: PEP-II LER expected modal growth rates vs. mode frequency ($l\omega_o + \omega_s$) at $I_o = 1$ A for: a) Even fill at nominal 8.4 ns spacing (feedback required). b) Even fill at 3×8.4 ns spacing (stabilised by modulation coupling).

utilised to measure the eigenvalues (growth rates and coherent tune shifts) of all unstable EFEMs simultaneously. The measurement technique is described in [17]. In most cases, only two of the 328 ALS modes were unstable: modes 204 and 233. The effective impedance at $233f_o$ was used to create a tune spread by maximising C_{233} (see Eq. (5)).

A baseline even-fill instability measurement was first made at $I_o = 172$ mA. This gave the following eigenvalues [25]: $\lambda_{204} = (0.47 \pm 0.02) - (0.05 \pm 0.03)j$ ms⁻¹ and $\lambda_{233} = (0.61 \pm 0.02) - (1.16 \pm 0.03)j$ ms⁻¹ (assuming that $d_r = 0.074$ ms⁻¹). It is evident from Fig. 3 that “Landau fills” with fill fractions less than 60% almost completely damp the primary target mode, which is EFEM 233 in this case. Thus, any residual instability in the Landau fill must correspond to the Landau-damped mode 204.

Although many methods exist for calculating the instability growth rate once the bunch tune distribution is calculated [14, 17], we use numerical computation of the eigenstructure of the mode coupling matrix, since it is the most exact. For this we need to know the shunt impedance R_s , the resonant frequency f_r and the quality factor Q of the two cavity modes responsible for the measured values of λ_{204} and λ_{233} . If the effective impedance corresponding to an even-fill eigenvalue is $R + jX$, then the shunt impedance R_s of the cavity mode obeys $(\frac{f_r}{f_r f} R_s - R)^2 + X^2 = [\frac{f_r}{f_r f} R_s]^2$ [17]. By correlating this result with data on ALS cavity modes [26], we get (nominally) $R_s = 11.36$ k Ω , $f_r = 1809.69$ MHz and $Q = 2900$ for EFEM 204 and $R_s = 43$ k Ω , $f_r = 2852.92$ MHz and $Q = 9149$ for EFEM 233. The numerical calculation then gives us an eigenvalue of $(0.1 \pm 0.04) + (1.62 \pm 0.06)j$ ms⁻¹ for the landau-damped mode 204. Error bars are calculated by assuming that errors in measured eigenvalues arise from fluctuations in f_r . Note: The real part of the most unstable eigenvalue is 6 times smaller than in the even-fill case. The measured eigenvalue for a 175-mA beam with $C_{233} = 0.67$ is $(0.09 \pm 0.003) + (1.63 \pm 0.005)j$ ms⁻¹, in agreement with the theoretical prediction.

4 SUMMARY

The use of phase space tracking as a new diagnostic for coupled-bunch instabilities has been demonstrated. As the PEP-II example shows, tracking facilitates more detailed comparisons between theory and experiment than conventional techniques. It is particularly useful in investigating complex phenomena such as two-stream instabilities. Other uses include accurate beam-based impedance measurement [27], quantification of the reactive component of active feedback, eigenmode analysis of uneven-fill motion [17], and (potentially) measurement of nonlinear effects such as tune variation with amplitude.

A systematic approach has been laid out for designing fill shapes that significantly damp coupled-bunch instabilities. The method, which is based on the phenomena of modulation coupling and fill-induced Landau damping, has been experimentally verified at the ALS and PEP-II, and also at SPEAR (see [17]). Instability cures based on these ideas are currently being studied at the SRRC [28].

Since mixing of oscillation-coordinate and fill-shape signals occurs in all planes, modulation coupling also affects transverse oscillations. Similarly, higher bunch-shape oscillations can also be damped by modulation coupling. Although bunches that are axially centered in the beam pipe induce no transverse steady-state wake, transverse Landau damping might be achieved by shifting the beam orbit (or a resonant structure) transversely.

Uneven-fill effects grow stronger as the maximum allowable bunch current i_{max} increases, and the beam current is distributed among fewer buckets. Uneven-fill cures for instabilities are thus limited by factors that limit i_{max} , such as heating of vacuum chamber elements, intrabunch scattering (beam lifetime) and beam-beam effects in colliders.

5 ACKNOWLEDGMENTS

I would like to thank A. Chao, S. Heifets, H. Hindi, G. Stupakov and D. Whittum of SLAC, A. Hofmann of CERN and M. Serio of INFN-LNF, B. Podobedov of BNL, C-X Wang of ANL and S. Bilbao and I. Linscott of Stanford University for helpful discussions. I am very grateful to A. Young of SLAC and G. Stover of LBNL for help with the measurements. This work was supported by DOE contract No. DE-AC03-76SF00515.

6 REFERENCES

- [1] A. Chao, *Physics of Collective Instabilities in High Energy Accelerators* (Wiley, 1993).
- [2] T. Raubenheimer and F. Zimmermann, *Phys. Rev. E* **52**, 5487 (1995).
- [3] G. Stupakov, T. Raubenheimer, and F. Zimmermann, *Phys. Rev. E* **52**, 5499 (1995).
- [4] F. Sacherer, *IEEE Trans. Nucl. Sci.* **20**, 825 (1973).
- [5] J. Laclare, in *11th International Conference on High Energy Accelerators*, Geneva, 1980, edited by W.S. Newman (Birkhauser Verlag, 1980), p. 526.
- [6] R.D. Kohaupt, DESY Report No. DESY 85-139, 1985.
- [7] S.A. Bogacz, *Part. Accel.* **48**, 19 (1994).
- [8] O. Naumann and J. Jacob, in *Proceedings of the 1997 Particle Accelerator Conference*, Vancouver (IEEE, 1998), p. 1551.
- [9] O. Meincke, CERN Report No. CERN-SL-98-018 (AP).
- [10] M. Billing, in *Proceedings of the 1997 Particle Accelerator Conference*, Vancouver (IEEE, 1998), p. 2317.
- [11] J. Sebek, private communication.
- [12] K. Harkay *et al.*, in *Proceedings of the 1997 Particle Accelerator Conference*, Vancouver (IEEE, 1998), p. 1575.
- [13] S. Prabhakar *et al.*, in *Beam Instrumentation Workshop*, proceedings of the 8th, Stanford, 1998, edited by R. Hettel, S. Smith, and J. Masek (AIP, 1999), p. 529.
- [14] H.G. Hereward, in *Proceedings of the CERN Accelerator School: Advanced Accelerator Physics*, Oxford, 1985, CERN 87-03, p. 255 (1987); Y.H. Chin and K. Yokoya, DESY Report No. DESY 86-097, 1986.
- [15] J.D. Fox *et al.*, in *Proceedings of the 1999 Particle Accelerator Conference* (IEEE, 1999), p. 636;
- [16] D. Teytelman *et al.*, in *Beam Instrumentation Workshop*, proceedings of the 8th, Stanford, 1998, edited by R. Hettel, S. Smith, and J. Masek (AIP, 1999), p. 222.
- [17] S. Prabhakar, Ph.D. thesis, Stanford University, 2000 (SLAC-R-554).
- [18] S. Prabhakar *et al.*, *Phys. Rev. ST Accel. Beams* **2**: 084401, 1999.
- [19] G. Stupakov, in *Proceedings of the 1997 Particle Accelerator Conference*, Vancouver (IEEE, 1998), p. 1632.
- [20] M. Minty *et al.*, in Tsukuba 1999, Performance Improvement of Electron-Positron Collider Particle Factories, proceedings of the international workshop, edited by K. Akai and E. Kikutani, 2000, p. 160.
- [21] E. Courant and A. Sessler, *Rev. Sci. Instrum.* **37**, 1579 (1966); K. Thompson and R.D. Ruth, in *1989 IEEE Particle Accelerator Conference: Accelerator Science and Technology* (IEEE, 1989), p. 792.
- [22] S. Prabhakar, J.D. Fox and D. Teytelman, *Phys. Rev. Lett.* **86**, 2022 (2001).
- [23] This is valid if $2\omega_s$ is much less than the bandwidth $\Delta\omega$ of the impedance resonance, since $Z^{eff}(-\omega) = -Z^{eff*}(\omega)$. On the other hand, if $\Delta\omega \ll 2\omega_s$, then $\lambda_{-n} \approx 0$, and EFEM n is damped just like the other modes.
- [24] R. Rimmer *et al.*, in *Fifth European Particle Accelerator Conference, Sitges, 1996*, edited by S. Myers *et al.* (Institute of Physics Publishing, 1996), p. 2035.
- [25] If the impedance is constant, eigenvalues vary linearly with I_o . Deviations from linearity arise from fluctuations in cavity temperatures and tuner positions, and from measurement noise. RMS deviations from linearity are used as error bars for eigenvalue measurements.
- [26] J. Corlett and J. Byrd, in *1993 IEEE Particle Accelerator Conference*, proceedings, Washington, D.C. (IEEE, 1994), p. 3408.
- [27] D. Teytelman *et al.*, these proceedings.
- [28] M.H. Wang, P.J. Chou and A. Chao, these proceedings.